

# An analysis of the magnetic behavior of olivine and garnet substitutional solid solutions <sup>♠</sup>

CHARLES A. GEIGER<sup>1,\*†</sup>, MICHAEL GRODZICKI<sup>1</sup>, AND EDGAR DACHS<sup>1</sup>

<sup>1</sup>Department Chemistry and Physics of Materials, Salzburg University, Jakob Haringer Strasse 2a, A-5020 Salzburg, Austria

## ABSTRACT

The low-temperature magnetic properties and Néel temperature,  $T_N$ , behavior of four silicate substitutional solid solutions containing paramagnetic ions are analyzed. The four systems are: fayalite-forsterite olivine [ $\text{Fe}_x^{2+}\text{SiO}_4\text{-Mg}_{2-x}\text{SiO}_4$ ], and the garnet series, grossular-andradite [ $\text{Ca}_3(\text{Al}_x\text{Fe}_{1-x}^{3+})_2\text{Si}_3\text{O}_{12}$ ], grossular-spessartine [ $(\text{Ca}_x\text{Mn}_{1-x}^{2+})_3\text{Al}_2\text{Si}_3\text{O}_{12}$ ], and almandine-spessartine [ $(\text{Fe}_x^{2+}\text{Mn}_{1-x}^{2+})_3\text{Al}_2\text{Si}_3\text{O}_{12}$ ]. Local magnetic behavior of the transition-metal-bearing end-members is taken from published neutron diffraction results and computational studies.  $T_N$  values are from calorimetric heat capacity,  $C_p$ , and magnetic susceptibility measurements. These end-members, along with more transition-metal-rich solid solutions, show a paramagnetic to antiferromagnetic phase transition. It is marked by a  $C_p$   $\lambda$ -anomaly that decreases in temperature and magnitude with increasing substitution of the diamagnetic component. For olivines,  $T_N$  varies between 65 and 18 K and  $T_N$  for the various garnets is less than 12 K. Local magnetic behavior can involve one or more superexchange interactions mediated through oxygen atoms.  $T_N$  behavior shows a quasi-plateau-like effect for the systems fayalite-forsterite, grossular-andradite, and grossular-spessartine. More transition-metal-rich crystals show a stronger  $T_N$  dependence compared to transition-metal-poor ones. The latter may possibly show superparamagnetic behavior.  $(\text{Fe}_x^{2+}\text{Mn}_{1-x}^{2+})_3\text{Al}_2\text{Si}_3\text{O}_{12}$  garnets show fundamentally different magnetic behavior. End-member almandine and spessartine have different and complex interacting local superexchange mechanisms and intermediate compositions show a double-exchange magnetic mechanism. For the latter,  $T_N$  values show negative deviations from linear interpolated  $T_N$  values between the end-members. Double exchange seldom occurs in oxides, and this may be the first documentation of this magnetic mechanism in a silicate.  $T_N$  behavior may possibly be used to better understand the nature of macroscopic thermodynamic functions,  $C_p$  and  $S^\circ$ , of both end-member and substitutional solid-solution phases.

**Keywords:** Olivine, garnet, heat capacity, Néel temperature, calorimetry, solid solutions, transition metals, superexchange, superparamagnetism, double exchange, thermodynamics; Isotopes, Minerals, and Petrology: Honoring John Valley

## INTRODUCTION

The majority of rock-forming minerals contains transition metals. Iron,  $\text{Fe}^{2+}$  and/or  $\text{Fe}^{3+}$ , is the most abundant element in terms of concentration, but  $\text{Ni}^{2+}$ ,  $\text{Mn}^{2+/3+}$ ,  $\text{Cr}^{3+}$ , and  $\text{Ti}^{4+}$  can also be considered major elements in some cases. Transition metals, even in small concentration, can play a key role in determining optical, magnetic, and various transport properties in crystals. Thermodynamic behavior can also be affected by them. Their presence affects large-scale Earth processes as in redox reactions and deep mantle melting, for example. The property of paleomagnetism is based on the ability of a mineral to retain a memory of Earth's paleogeomagnetic field during crystallization.

At the simplest level, magnetism in minerals results from partially occupied  $d$ -shells of transition-metal ions (minerals with  $f$  electrons can also be magnetic, but for rock-forming minerals these electrons are less important in terms of magnetic behavior). The resulting physical property is a magnetic dipole moment generated by the spin of the electrons. In terms of classical physics, the spin can be described by an electron spinning in either a clockwise or counterclockwise (or spin up and spin down) manner.

In quantum terms, this is given by the spin quantum number, where  $M_S = +\frac{1}{2}$  or  $M_S = -\frac{1}{2}$ . Magnetic behavior in crystals is determined by the type and strength of the various interactions between the electron spins. These interactions can be of the simple dipole type or more complex ones involving additional intervening atoms (Goodenough 1963; Blundell 2001). All spin interactions are a function of temperature.

Detailed study of the magnetic behavior of crystals in the mineralogical sciences is relatively young (see Parks and Akhtar 1968, for an early work and references therein) and not extensive. In contrast, in physics and material sciences the amount of research made on the magnetic behavior of crystals is enormous. In the late 1940s, important theoretical concepts were developed, synthesis experiments on various composition spinel(ferrite)- and garnet-structure crystals were started and investigations on their magnetic properties were made (e.g., Néel 1948; Geller 1967; Winkler 1981). Many of these phases contain rare earth elements with partially occupied  $f$ -orbitals, but  $\text{Fe}^{2+,3+}$  with  $d$ -electrons is important in many cases.

In contrast, little study has focused on the magnetic properties of rock-forming silicates and especially for substitutional solid solutions. The level of scientific understanding is minimal to nonexistent. In these systems, the electronic configuration of the transition metal(s), its/their structural location and concentration in a crystal are critical, because they together will determine the

\* E-mail: ca.geiger@sbg.ac.at

<sup>♠</sup> Open access: Article available to all readers online. This article is CC-BY-NC-ND.

<sup>†</sup> Special collection papers can be found online at <http://www.minsocam.org/MSA/AmMin/special-collections.html>.

type of magnetic interaction(s). Fayalite,  $\text{Fe}_2^+\text{SiO}_4$ , and fayalite-forsterite,  $\text{Fe}_2^+\text{SiO}_4\text{-Mg}_2\text{SiO}_4$ , olivine substitutional solid solutions have received the most attention. Fayalite shows a large and relatively high-temperature magnetic transition at about 65 K, but magnetic behavior at lower temperatures down to roughly 20 K is controversial (e.g., Santoro et al. 1966; Robie et al. 1982; Lottermoser et al. 1986; Aronson et al. 2007). With increasing the forsterite component in  $\text{Fe}^{2+}$ -Mg olivine substitutional solid solutions, the magnetic transition temperature decreases (Dachs et al. 2007; Belley et al. 2009). The common end-member silicate garnets, almandine (Prandl 1971; Murad and Wagner 1987; Anovitz et al. 1993; Dachs et al. 2014b), spessartine (Prandl 1973; Dachs et al. 2009; Lau et al. 2009), and andradite (Murad 1984; Plakhty et al. 1993; Geiger et al. 2018) have been investigated and they undergo a very low temperature ( $T < 12$  K) spin transition. The transition in both silicate structure types of end-member composition is of the paramagnetic-antiferromagnetic type marking a disordered to a long-range ordered spin state. It is defined by the Neel temperature,  $T_N$ , which in terms of experimental  $C_p$  measurements is expressed by a  $\lambda$ -anomaly.

We undertook an analysis of the magnetic behavior of the fayalite-forsterite and three garnet binary substitutional solid solutions, namely grossular-andradite,  $\text{Ca}_3(\text{Fe}_x^3+\text{Al}_{1-x})_2\text{Si}_3\text{O}_{12}$ , grossular-spessartine,  $(\text{Ca}_x\text{Mn}_{1-x}^{2+})_3\text{Al}_2\text{Si}_3\text{O}_{12}$ , and almandine-spessartine,  $(\text{Fe}_x^2+\text{Mn}_{1-x}^{2+})_3\text{Al}_2\text{Si}_3\text{O}_{12}$ . A knowledge of  $T_N$  behavior across a given binary join, as determined by low-temperature calorimetry or magnetic susceptibility measurements, together with an understanding of the local magnetic properties of the one or two paramagnetic end-members, as determined via neutron diffraction and/or calculations, allows the magnetic behavior as a function of composition to be analyzed. This type of study has not been done before. Furthermore, an analysis of magnetic behavior can help better understand crystal-chemical and macroscopic thermodynamic properties.

### SAMPLES AND LOW-TEMPERATURE CALORIMETRY

The synthesis conditions or the natural localities for the various crystals of the four binary solid solutions, along with their chemical and physical characterization, have already been described in different publications. The four systems and cited descriptions, discussing the synthesis and characterization measurements, are: (1) fayalite-forsterite,  $\text{Fe}_2^+\text{SiO}_4\text{-Mg}_2\text{SiO}_4$ , olivine (von Seckendorff and O'Neill 1993), (2) grossular-andradite,  $\text{Ca}_3(\text{Al}_x\text{Fe}_{3-x}^3)\text{Si}_3\text{O}_{12}$  (Geiger et al. 2018; Dachs and Geiger 2019), (3) grossular-spessartine,  $(\text{Ca}_x\text{Mn}_{1-x}^{2+})_3\text{Al}_2\text{Si}_3\text{O}_{12}$  (Geiger 2000; Rodehorst et al. 2004), and (4) almandine-spessartine,  $(\text{Fe}_x^2+\text{Mn}_{1-x}^{2+})_3\text{Al}_2\text{Si}_3\text{O}_{12}$  (Geiger 2000; Geiger and Rossman 1994; Geiger and Feenstra 1997). The various samples are better than about 99% phase pure.

The low-temperature (i.e., 2 or 5 to 300 K) heat capacity,  $C_p$ , of the various crystals was measured previously with the Physical Properties Measurement System constructed by Quantum Design. The calorimetric method and measurement setup have been discussed numerous times (Dachs et al. 2009, 2012, 2014a, 2014b; Geiger and Dachs 2018; Geiger et al. 2018; Dachs and Geiger 2019) and will not be repeated here.

### EXPERIMENTAL RESULTS

Low-temperature  $C_p$  behavior for synthetic olivines across the  $\text{Fe}_2^+\text{SiO}_4\text{-Mg}_2\text{SiO}_4$  binary is shown in Dachs et al. (2007). The magnetic transitions and their various

$T_N$  values are shown and given, respectively, in this work. The behavior of  $T_N$  across the  $\text{Fe}_2^+\text{SiO}_4\text{-Mg}_2\text{SiO}_4$  binary, as determined by the low-temperature  $C_p$  and also by magnetic susceptibility (Belley et al. 2009) measurements, is shown in Figure 1 and Figure 1a, respectively.  $T_N$  values are listed in Table 1.

The low-temperature  $C_p$  behavior for end-member andradite and solid-solution  $\text{Ca}_3(\text{Al}_x\text{Fe}_{3-x}^3)\text{Si}_3\text{O}_{12}$  garnets are shown in Geiger et al. (2018) and Dachs and Geiger (2019). The low-temperature  $C_p$  behavior for spessartine and  $(\text{Ca}_x\text{Mn}_{1-x}^{2+})_3\text{Al}_2\text{Si}_3\text{O}_{12}$  garnets are shown in Dachs et al. (2009) and Dachs et al. (2014a) and for almandine and  $(\text{Fe}_x^2+\text{Mn}_{1-x}^{2+})_3\text{Al}_2\text{Si}_3\text{O}_{12}$  garnets in Dachs et al. (2012) and Dachs et al. (2014b). The behavior of  $T_N$  for all three garnet binaries is displayed in Figure 2.  $T_N$  values are listed in Table 1.

Analyses of the  $C_p$  results, in terms of modeling the magnetic transitions and the determination of  $T_N$ , are discussed at length in the cited investigations.  $T_N$  is given by the peak temperature of the magnetic  $\lambda$ -anomaly.

## DISCUSSION

### Heat-capacity measurements and brief theory on magnetism

Thermophysical properties of crystals, including magnetic behavior, can change greatly in the vicinity of the critical temperature of a transition. The subject is broad and complex and cannot be treated here (see Gopal 1966; Grimvall 1986). Suffice it to note that heat-capacity measurements, where  $C_p = (dH/dT)_p$  and  $H$  is the enthalpy, afford an excellent means of studying  $T_N$  and magnetic behavior of crystals (e.g., Stout 1961; Gopal 1966). In the case of most silicates studied to date, magnetic transitions occur below 65 K (i.e., fayalite) and usually at much lower temperatures. Thus, the magnetic interactions are weak, but in some cases they can give rise to larger  $C_p(T)$  values than those deriving from atomic vibrations (phonons) at low temperatures. When it is possible to separate the vibrational (phonon or lattice) heat capacity,  $C_{\text{vib}}$ , from the magnetic heat capacity,  $C_{\text{mag}}$ ,

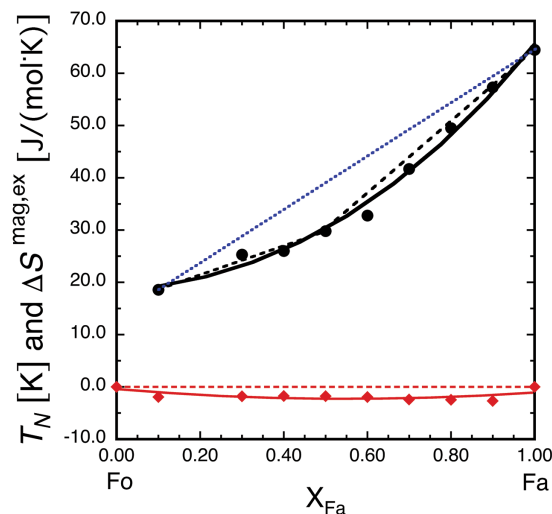


**FIGURE 1.** Néel temperature,  $T_N$ , behavior for fayalite-forsterite,  $\text{Fe}_2^+\text{SiO}_4\text{-Mg}_2\text{SiO}_4$ , olivines (Fa = fayalite and Fo = forsterite). The solid black points give  $T_N$  for each olivine composition (errors in  $T_N$  are discussed in the text). The data can be described by two linear segments (black dashed lines) or a third-order polynomial (solid black line). The blue dashed line connects  $\text{Fa}_{100}$  and  $\text{Fa}_{10}\text{Fo}_{90}$ . At the bottom of the figure, values for the excess magnetic entropy of mixing for different composition olivines are given by the red diamonds (Dachs et al. 2007). The solid red line represents a third-order polynomial fit to the data. The dashed red line represents ideal magnetic entropy of mixing behavior.

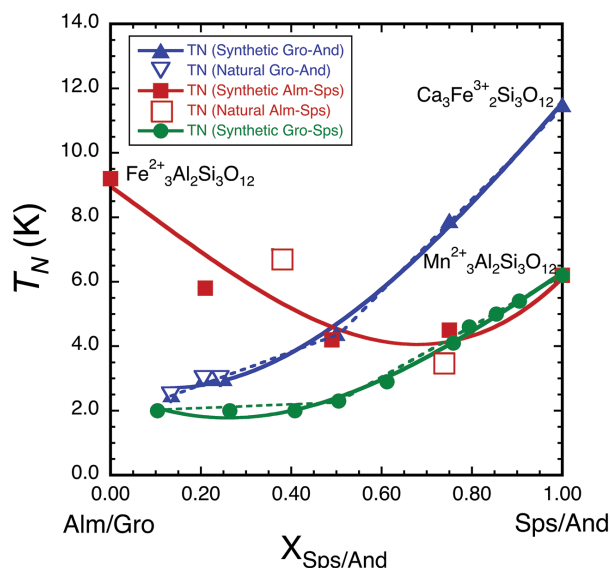


**FIGURE 2.** Néel temperature,  $T_N$ , behavior for three garnet binary substitutional solid solutions. (a) Grossular-andradite that is  $\text{Ca}_3(\text{Al}_x\text{Fe}_{1-x}^{3+})_2\text{Si}_3\text{O}_{12}$ . (b) Grossular-spessartine that is  $(\text{Ca}_x\text{Mn}_{1-x}^{2+})_3\text{Al}_2\text{Si}_3\text{O}_{12}$ . (c) Almandine-spessartine that is  $(\text{Fe}_x^{2+}\text{Mn}_{1-x}^{2+})_3\text{Al}_2\text{Si}_3\text{O}_{12}$ . (Alm = almandine, Sps = spessartine, Gro = grossular, and And = andradite). The two dashed lines show linear-segment fits to the respective data. The solid curves represent third-order polynomial fits.

from experimental  $C_p$  measurements important information is obtained (e.g., Gopal 1966).

Experimental investigations of different types made on transition-metal-bearing olivines and garnets demonstrate that these two structure types undergo one or two magnetic or magnetic-related transitions at low temperatures. In terms of calorimetry, it is marked by a  $\lambda$ -peak or  $\lambda$ -anomaly (i.e., second-order phase transition) that describes the thermophysical changes resulting from the magnetic interactions, whereby disordered electron spins begin to interact locally and order with decreasing temperature. The start of spin ordering (short range) coincides with the onset of the high-temperature flank of the  $\lambda$ -peak until reaching a completely long-range ordered state at the critical temperature of  $T_N$ .

According to the Heisenberg model for interacting localized

spins, the effective magnetic coupling constant,  $J_{\text{eff}}$  (any given energy unit, for example, K), is related to  $T_N$  by the relationship:

$$\frac{J_{\text{eff}}}{k} = \frac{3T_N}{zS(S+1)} \quad (1)$$

where  $k$  is the Boltzmann constant,  $S$  is the total spin, and  $z$  is the number of nearest neighbor magnetic ions [ $z = 2$  (M1) and 4 (M2) for olivine and  $z = 4$  (dodecahedral site) or 6 (octahedral site) for garnet]. On the basis of accurate crystal-structure results, the magnetic coupling constant,  $J$ , for two weakly coupled localized spins  $S^A$  and  $S^B$  can be obtained from the energy difference between parallel ( $S_{\text{max}}$ ) and antiparallel ( $S_{\text{min}}$ ) alignment of the spins (Zhebrebetsky et al. 2012 and references therein). It is given by:

$$J = -\frac{E(S_{\text{max}}) - E(S_{\text{min}})}{S_{\text{max}}^2 - S_{\text{min}}^2} \quad (2)$$

where the numerically calculated  $E(S)$  is the total energy for the spin state,  $S$ . Positive values of  $J$  correspond to parallel or ferromagnetic and negative values to antiparallel or antiferromagnetic coupling of the two spins  $S^A$  and  $S^B$ .

### Olivine and garnet crystal structures

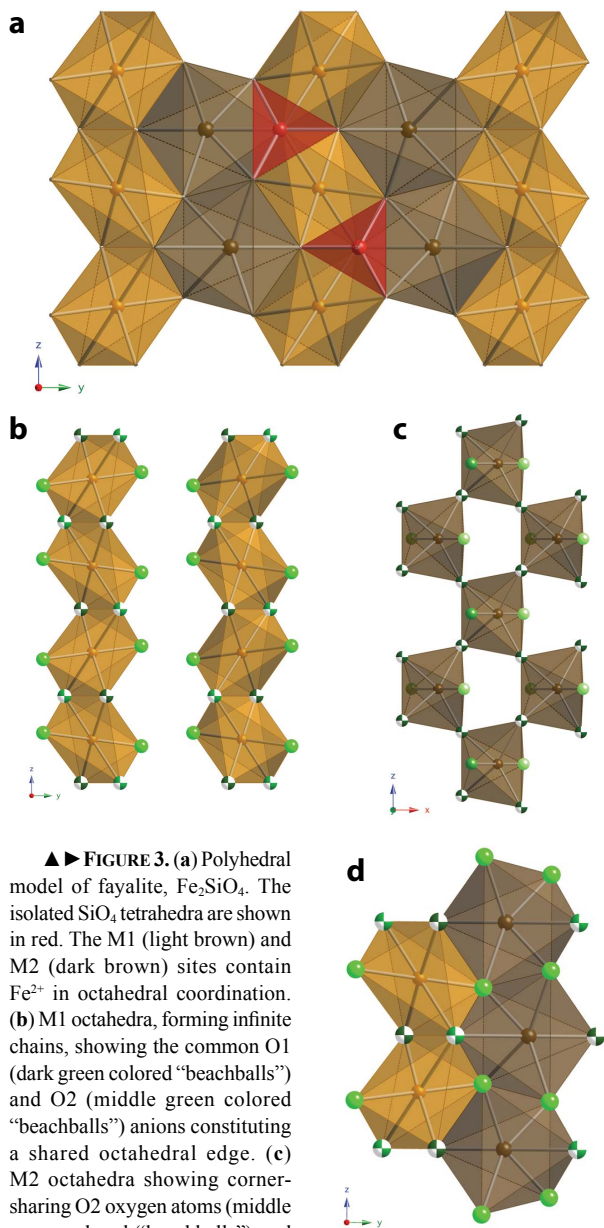
**Olivine.** Olivine,  $X_2\text{SiO}_4$ , with  $X = \text{Fe}^{2+}$  (fayalite) and/or Mg (forsterite), is crystallographically orthorhombic with space group  $Pbnm$ , and it has 4 formula units per unit cell. The crystal structure is shown in Figure 3. The two crystallographically independent cation sites, excluding Si, are termed  $M1$  and  $M2$ .  $M2$ , Si, O1, and O2 atoms are located on mirror planes and have  $m$  point symmetry. The  $M1$  cation is located at the origin of the unit cell and has  $\bar{1}$  point symmetry, while O3 and O4 occupy general positions of symmetry 1. Several structural and crystal-chemical studies investigated the nature of the long-range Mg-Fe $^{2+}$  distribution over the two  $M1$  and  $M2$  octahedral sites in  $\text{Fe}_2^{2+}\text{SiO}_4$ - $\text{Mg}_2\text{SiO}_4$  solid solutions. There are contradictory results and interpretations obtained over the years. The careful, recent X-ray diffraction investigation of Heinemann et al. (2007) summarizes the situation on order-disorder.

**Garnet.** The garnet crystal structure, space group  $Ia\bar{3}d$ , general formula  $\{X_3\}[Y_2](Z_3)\text{O}_{12}$ , contains three different and independent cation sites (Menzer 1928; Novak and Gibbs 1971) forming a quasi-framework consisting of rigid corner-sharing  $\text{ZO}_4$  tetrahedra and  $\text{YO}_6$  octahedra (Armbruster et al. 1992). There are eight formula units per unit cell. The structure is shown in Figure 4a. The  $Y$ -cations are located at the Wyckoff site  $16d$  of point sym-

**TABLE 1.** Neel temperature,  $T_N$ , for various composition phases for synthetic olivine and three garnet binary solid solutions as determined by relaxation calorimetry and magnetic susceptibility measurements

Olivine	$T_N^a$	$T_N^b$	Garnet <sup>c</sup>	$T_N$	Garnet <sup>d</sup>	$T_N$	Garnet <sup>e,f</sup>	$T_N$
Fa <sub>100</sub>	64.5(1)	67	Alm <sub>100</sub>	9.2	Gro <sub>100</sub>	–	Gro <sub>100</sub>	–
Fa <sub>90</sub> FO <sub>10</sub>	57.3(1)	59	Alm <sub>75</sub> Sps <sub>25</sub>	5.8	Gro <sub>90</sub> Sps <sub>10</sub>	<2	Gro <sub>75</sub> And <sub>25</sub>	3.0
Fa <sub>80</sub> FO <sub>20</sub>	49.5(1)	55	Alm <sub>50</sub> Sps <sub>50</sub>	4.2	Gro <sub>75</sub> Sps <sub>25</sub>	<2	Gro <sub>50</sub> And <sub>50</sub>	4.4
Fa <sub>70</sub> FO <sub>30</sub>	41.7(1)	45	Alm <sub>25</sub> Sps <sub>75</sub>	4.5	Gro <sub>60</sub> Sps <sub>40</sub>	<2	Gro <sub>25</sub> And <sub>75</sub>	7.9
Fa <sub>60</sub> FO <sub>40</sub>	32.8(1)	33	Sps <sub>100</sub>	6.2	Gro <sub>50</sub> Sps <sub>50</sub>	2.3	And <sub>100</sub>	11.5
Fa <sub>50</sub> FO <sub>50</sub>	29.8	21			Gro <sub>40</sub> Sps <sub>60</sub>	2.9		
Fa <sub>40</sub> FO <sub>60</sub>	26.0	20			Gro <sub>25</sub> Sps <sub>75</sub>	4.1		
Fa <sub>30</sub> FO <sub>70</sub>	25.3	–	<sup>g,h</sup> Alm <sub>75</sub> Sps <sub>26</sub>	6.7	Gro <sub>20</sub> Sps <sub>80</sub>	4.6	<sup>g,i</sup> Gro <sub>82</sub> And <sub>13</sub>	2.5
Fa <sub>20</sub> FO <sub>80</sub>	–	–	<sup>g,h</sup> Alm <sub>36</sub> Sps <sub>62</sub>	3.5	Gro <sub>15</sub> Sps <sub>85</sub>	5.0	<sup>g,i</sup> Gro <sub>74</sub> And <sub>19</sub>	3.0
Fa <sub>10</sub> FO <sub>90</sub>	18.6	–			Gro <sub>10</sub> Sps <sub>90</sub>	5.4	<sup>g,i</sup> Gro <sub>73</sub> And <sub>23</sub>	3.0
FO <sub>100</sub>	–	–			Sps <sub>100</sub>	6.2		

Notes: Fa = fayalite, Fo = forsterite, Alm = almandine, Sps = spessartine, Gro = grossular, And = andradite.  $T_N$  values synthetic olivine: <sup>a</sup>Dachs et al. (2007) and <sup>b</sup>Belley et al. (2009).  $T_N$  values: synthetic and <sup>g</sup>natural (extra minor elements not considered) garnet: <sup>c</sup>Dachs et al. (2012, 2014b), <sup>d</sup>Dachs et al. (2014a), <sup>e</sup>Geiger et al. (2018), and <sup>f</sup>Dachs and Geiger (2019). The given compositions are nominal. See cited papers under "Samples and Low-temperature Calorimetry" for more detailed information as well as <sup>h</sup>Geiger and Rossman (1994) and <sup>i</sup>Dachs and Geiger (2019).



▲► **FIGURE 3.** (a) Polyhedral model of fayalite,  $\text{Fe}_2\text{SiO}_4$ . The isolated  $\text{SiO}_4$  tetrahedra are shown in red. The M1 (light brown) and M2 (dark brown) sites contain  $\text{Fe}^{2+}$  in octahedral coordination. (b) M1 octahedra, forming infinite chains, showing the common O1 (dark green colored “beachballs”) and O2 (middle green colored “beachballs”) anions constituting a shared octahedral edge. (c) M2 octahedra showing corner-sharing O2 oxygen atoms (middle green colored “beachballs”) and unshared O1 (solid middle green spheres) and O3 (solid bright green spheres) O atoms. (d) M1 and M2 octahedral showing common edge-shared O3 (bright green colored “beachballs”) and O2 oxygen atoms (middle green colored “beachballs”).

metry  $\bar{3}$ . The  $X$ -cations, located at  $24c$  of point symmetry  $222$ , are coordinated by 8 oxygen atoms in the form of a triangular dodecahedron. All sites allow for the incorporation of various cations with or without unpaired  $d$ - or  $f$ -electrons (Winkler 1981), whereby the major cations for the common silicate garnets ( $Z = \text{Si}$  of point symmetry  $\bar{4}$ ) are  $X = \text{Ca}, \text{Mg}, \text{Fe}^{2+}, \text{and Mn}^{2+}$  and  $Y = \text{Al}, \text{Fe}^{3+}, \text{and Cr}^{3+}$ . Accordingly, magnetic interactions can occur on two different sublattices that can, furthermore, interact with each other leading to varying magnetic behavior depending on the garnet chemistry. The occurrence of solid solutions, which can be

extensive, of varying compositions can lead to significant changes in the physical properties of garnet (Geiger 2013).

### Magnetic and $T_N$ behavior in olivine and garnet solid solutions: Binary systems with a paramagnetic and diamagnetic end-member

**$\text{Fe}_2^{2+}\text{SiO}_4$ - $\text{Mg}_2\text{SiO}_4$  olivines.** Paramagnetic fayalite shows a magnetic transition at 65 K, as measured experimentally several times (e.g., Santoro et al. 1966; Robie et al. 1982; Lottermoser et al. 1986; Aronson et al. 2007). Müller et al. (1982) investigated the magnetic structure of synthetic fayalite using unpolarized neutron diffraction data recorded at 4.2, 35, and 120 K. The results show that the electronic and magnetic properties deriving from the two crystallographically independent  $\text{Fe}^{2+}$  atoms at M1 and M2 are complex. Magnetic interactions occur on the two different sublattices that interact, furthermore, between each other. The ab initio calculations of Cococcioni et al. (2003) for the ground state of fayalite were interpreted as showing that ferromagnetic spin ordering occurs between edge-sharing octahedra (Figs. 3b and 3d) and antiferromagnetic ordering occurs between corner-sharing octahedra (Fig. 3c) and both through oxygen-mediated superexchange.

Forsterite is diamagnetic, but all studied forsterite-containing  $\text{Fe}_2^{2+}\text{SiO}_4$ - $\text{Mg}_2\text{SiO}_4$  solid solutions show a “ $\lambda$ -anomaly.”  $T_N$  decreases with increasing forsterite component in the olivine as observed via calorimetry (Dachs et al. 2007) and magnetic susceptibility measurements (Belley et al. 2009). This behavior is shown in Figure 1 and Supplemental<sup>1</sup> Figure 1a (see data in Table 1). The intensity of the  $C_p \lambda$ -peak also decreases accordingly.  $T_N$  values obtained via magnetic susceptibility measurements on fayalite-rich olivines are in good agreement with those obtained from calorimetry. There are greater differences for  $\text{Fa}_{50}\text{Fo}_{50}$  and  $\text{Fa}_{40}\text{Fo}_{60}$  compositions. Belley et al. (2009) did not observe a transition in more forsterite-rich olivines. (Note: The errors in  $T_N$  are considered to be larger than those in Dachs et al. (2007), Table 1).

In terms of calorimetric determinations,  $T_N$  is 65 K for fayalite and  $T_N$  decreases to 18.6 K for composition  $\text{Fa}_{10}\text{Fo}_{90}$ .  $T_N$  behavior across the binary join can be described with two linear segments with a break around composition  $\text{Fa}_{50}\text{Fo}_{50}$ . One segment is given by the  $T_N$  values from  $\text{Fa}_{100}$  to about  $\text{Fa}_{50}\text{Fo}_{50}$ , while the other segment describes  $T_N$  values from about  $\text{Fa}_{50}\text{Fo}_{50}$  to  $\text{Fa}_{10}\text{Fo}_{90}$ . For the latter, the change in  $T_N$  is less compositionally dependent. All the  $T_N$  data across the binary can also be fit by a third-order polynomial (Fig. 1).

**$\text{Ca}_3(\text{Al}, \text{Fe}_{1-x}^{3+})_2\text{Si}_3\text{O}_{12}$  garnets.** Paramagnetic andradite contains one transition-metal per formula unit, namely  $\text{Fe}^{3+}$ , and it is located at the  $16a$  octahedral site (Figs. 4a, 4b, and 4c). Plakhty et al. (1993) analyzed the nature of the magnons and magnetic exchange interactions in a natural nearly end-member andradite containing a small amount of  $\text{Mn}^{2+}$  and  $\text{Al}^{3+}$ , as well as in isostructural synthetic  $\text{Ca}_3\text{Fe}_2^{3+}\text{Ge}_3\text{O}_{12}$ , from inelastic neutron scattering measurements made at 4.2 K. The strongest interactions derive from  $\text{Fe}^{3+}(3d^5)$ . These workers concluded that magnetic superexchange occurred through the  $p_o$  orbitals of intermediate oxygen atoms across octahedral-dodecahedra,  $\text{Fe}^{3+}\text{-O}(\text{Ca})\text{-O-Fe}^{3+}$  bridges (Fig. 4c). Meyer et al. (2010) investigated, furthermore, the local magnetic coupling mechanisms between  $\text{Fe}^{3+}$  atoms in  $\text{And}_{100}$  using ab initio methods. They proposed that the low-temperature

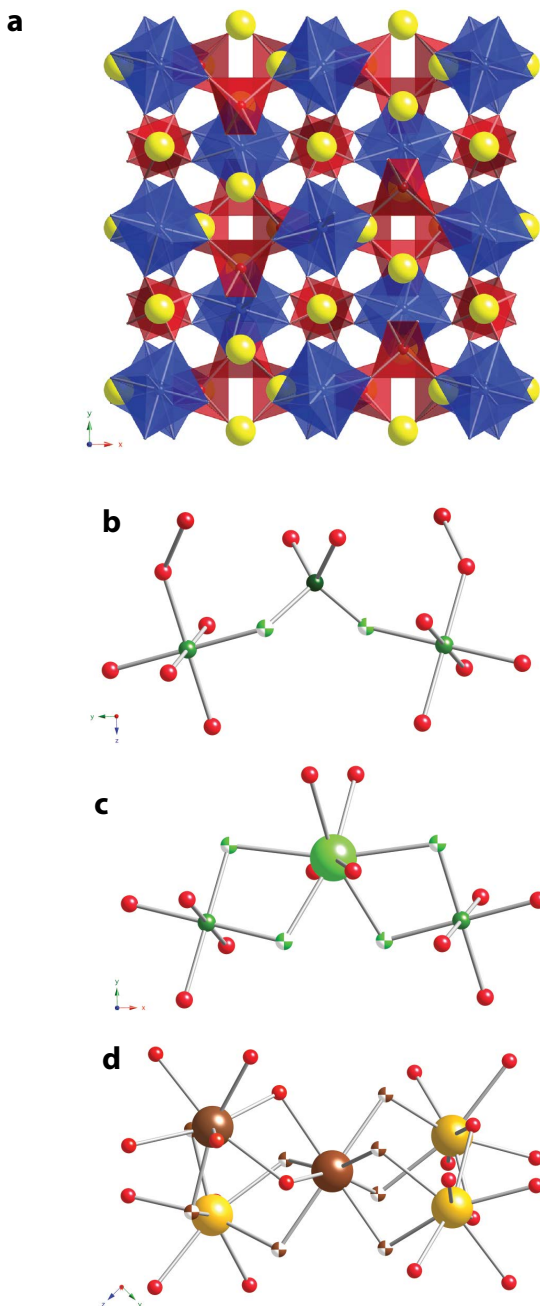


**FIGURE 4.** (a) Polyhedral model of silicate garnet. The  $\text{SiO}_4$  tetrahedra and  $\text{AlO}_6$  octahedra share corners, building a quasi-three-dimensional framework. The  $X$  cations (yellow spheres) are located in small cavities of triangular dodecahedron coordination. (b) In andradite two  $\text{Fe}^{3+}\text{O}_6$  octahedra with  $\text{Fe}^{3+}$  given by the medium-colored green spheres and a central  $\text{SiO}_4$  tetrahedron (Si cation dark green). One local superexchange bridge is given by the green colored cations (Meyer et al. 2010) and the oxygen anions by “beachball” spheres via  $\text{Fe}^{3+}\text{-O-(Si)-O-Fe}^{3+}$ . (c) A second possible superexchange in andradite is given by  $\text{Fe}^{3+}\text{-O-(Ca)-O-Fe}^{3+}$  bridges (Meyer et al. 2010). The Ca atom is shown as the large light green sphere. (d) One possible relationship between neighboring edge-sharing  $\text{XO}_6$  groups for a given almandine-spessartine solid solution ( $\text{Fe}^{2+}$  = dark brown and  $\text{Mn}^{2+}$  = light brown). “Normal” ferromagnetic superexchange occurs through oxygen anions Zherebetsky et al. (2012). Double exchange occurs through the “beachball”-illustrated O atoms. Note that the relative sizes of the various ions are not correct but made to make the local magnetic interactions easier to visualize.

antiferromagnetic transition results from weak superexchange interactions via both  $\text{Fe}^{3+}\text{-O-(Si)-O-Fe}^{3+}$  and  $\text{Fe}^{3+}\text{-O-(Ca)-O-Fe}^{3+}$  bridges (Figs. 4b and 4c).

The two different local interactions may possibly be expressed in the  $C_p$  behavior of end-member andradite (Geiger et al. 2018). Here, the “ $\lambda$ -peak” appears to show a shoulder on its low-temperature flank (Fig. 5), which is even more pronounced in terms of entropy behavior at these low temperatures—as given by  $S(T) = \int (C_p/T)dT$  (Geiger and Dachs 2018). The shorter superexchange bridge [i.e.,  $\text{Fe}^{3+}\text{-O-(Si)-O-Fe}^{3+}$ ] should be marked by the higher temperature maximum intensity of the “ $\lambda$ -peak” at  $11.3 (\pm 0.2)$  K and the longer and weaker superexchange interaction [i.e.,  $\text{Fe}^{3+}\text{-O-(Ca)-O-Fe}^{3+}$ ] by the low-temperature shoulder at  $\sim 5$  K. Modeling of the experimental  $C_p$  data to obtain  $C_{\text{mag}}$  shows that the high-temperature flank of the “ $\lambda$ -peak” extends above 11 K (Fig. 5). Therefore, some degree of spin ordering is expected at these temperatures. More research is needed to address the precise physical nature of the  $\lambda$ -peak in andradite.

Grossular is diamagnetic, but all studied andradite-containing  $\text{Ca}_3(\text{Al}_x\text{Fe}_{1-x})_2\text{Si}_3\text{O}_{12}$  solid solutions show a “ $\lambda$ -anomaly”.  $T_N$  decreases with increasing grossular component in the garnet from 11.3 K in  $\text{And}_{100}$  (Murad 1984; Geiger et al. 2018) to about 3 K for the most grossular-rich garnets roughly  $\text{Gro}_{80}\text{And}_{20}$  (Fig. 2 with  $T_N$  values given in Table 1). The intensity of the “ $\lambda$ -peak” also decreases with increasing grossular component in the garnet (Dachs and Geiger 2019). Both indicate a weakening of the local magnetic interactions. The  $T_N$  data across the join can be fit with two linear segments with a break occurring around  $\text{And}_{50}\text{Gro}_{50}$  (Fig. 2) or with a third-order polynomial.

**( $\text{Ca}_x\text{Mn}_{1-x}^{2+}$ ) $_3\text{Al}_2\text{Si}_3\text{O}_{12}$  garnets.** Paramagnetic spessartine contains one transition-metal cation per formula unit, namely  $\text{Mn}^{2+}$ , that is located at the 24c dodecahedral site (Fig. 4a). Prandl (1973) investigated the magnetic structure of synthetic spessartine using neutron powder data. Spessartine shows a  $\lambda$ -anomaly at  $T_N = 6.2$  K (Fig. 5, Dachs et al. 2009) and magnetic susceptibility measurements give a transition at 7 K (Lau et al. 2009). Short-range, but not long-range, spin ordering of

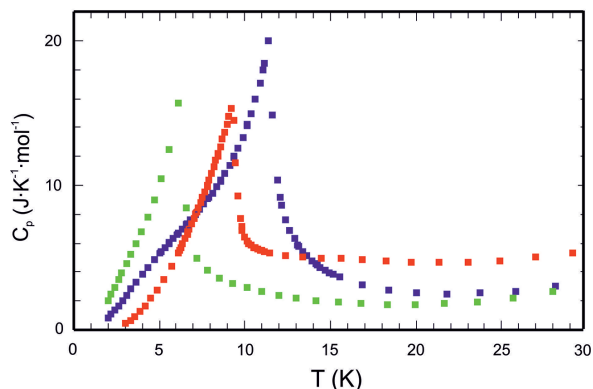


**FIGURE 5.**  $C_p(T)_{\text{mag}}$  behavior for almandine (red), spessartine (green), and andradite (blue) normalized to one transition-metal-cation. The three  $\lambda$ -peaks were obtained through calorimetric measurements (Dachs et al. 2009, 2012; Geiger et al. 2018).  $T_N$  is measurable to better than  $\pm 0.2$  K. Note the  $\lambda$ -peak for andradite and the presence of a weak shoulder on the low-temperature flank. Its origin is discussed in the text.

Mn<sup>2+</sup>(3d<sup>5</sup>) is present above this temperature.

As stated above, grossular is diamagnetic but all studied spessartine-containing (Ca<sub>x</sub>Mn<sup>2+</sup><sub>1-x</sub>)<sub>3</sub>Al<sub>2</sub>Si<sub>3</sub>O<sub>12</sub> solid solutions show a “λ-anomaly”. T<sub>N</sub> values for spessartine and (Ca<sub>x</sub>Mn<sup>2+</sup><sub>1-x</sub>)<sub>3</sub>Al<sub>2</sub>Si<sub>3</sub>O<sub>12</sub> solid-solution garnets are plotted in Figure 2 (values in Table 1). Starting from Sps<sub>100</sub> and moving to more grossular-rich garnets, T<sub>N</sub> decreases from 6.2 K to about 2.2 K for the Sps<sub>50</sub>Gro<sub>50</sub> composition. At grossular-rich compositions, T<sub>N</sub> shows a plateauing behavior with T<sub>N</sub> values ≤2.0 K (Table 1). A precise determination of T<sub>N</sub> for the most grossular-rich garnets is difficult due to their weak and broad λ-peaks. Moreover, our C<sub>p</sub> measurements can only be made down to 2 K. T<sub>N</sub> behavior across the join can, once again, be described using two linear segments or a third-order polynomial.

**Magnetic behavior as a function of composition.** All the experimental data on olivine show a decreasing and nonlinear behavior in T<sub>N</sub> across the Fe<sub>2</sub><sup>+</sup>SiO<sub>4</sub>-Mg<sub>2</sub>SiO<sub>4</sub> join. T<sub>N</sub>, marking a paramagnetic-antiferromagnetic transition, decreases from Fa<sub>100</sub> to Fa<sub>10</sub>Fo<sub>90</sub> with a quasi-plateauing behavior for forsterite-rich compositions. The magnetic structure in the fayalite-rich solid solutions should be governed, as in Fa<sub>100</sub> (Cococcioni et al. 2003), by superexchange interactions through oxygen among Fe<sup>2+</sup> cations (Figs. 3b, 3c, and 3d). A decrease in the intensity of the λ-peak as a function of composition also demonstrates a weakening of the local magnetic interactions.

Analogous T<sub>N</sub> behavior is observed for Ca<sub>3</sub>(Al<sub>x</sub>Fe<sup>3+</sup><sub>1-x</sub>)<sub>2</sub>Si<sub>3</sub>O<sub>12</sub> and (Ca<sub>x</sub>Mn<sup>2+</sup><sub>1-x</sub>)<sub>3</sub>Al<sub>2</sub>Si<sub>3</sub>O<sub>12</sub> garnets and the variation in magnetic properties could be similar to that in olivine. Andradite and spessartine transition to an antiferromagnetic state and this is also considered the case for andradite- and spessartine-rich solid solutions. For both binaries, T<sub>N</sub> shows a quasi-plateau-like effect, whereby T<sub>N</sub> is more strongly temperature dependent in garnets richer in paramagnetic cations compared to those richer in diamagnetic ones, namely Al<sup>3+</sup> and Ca<sup>2+</sup>, respectively.

T<sub>N</sub> for all three solid-solution binaries appears to exhibit a change in temperature dependence roughly around the 50:50 composition region. Notably, magnetic ordering persists in paramagnetically dilute solid solutions and in the case of olivine even for the Fe<sup>2+</sup>-poor composition Fa<sub>10</sub>Fo<sub>90</sub>. Superexchange is responsible for magnetic ordering in the transition-metal-bearing end-members, and as well, we think, for the magnetic-cation-rich compositions. However, it would appear to be difficult for superexchange to persist in compositions richer in the diamagnetic component, because superexchange is a local interaction, decreasing exponentially in strength with distance. The observed magnetic ordering in diamagnetic-component-rich solutions requires long-range interactions. What are the alternatives?

The first and most obvious one is dipolar interactions between randomly distributed isolated magnetic ions. An estimate of the order of magnitude of the magnetic energy, U<sub>mag</sub>, of the dipole interaction between two free Fe<sup>2+</sup> cations, for example, with (anti)parallel alignment is given by

$$\begin{aligned} |U_{\text{mag}}| &= \frac{2\mu_0\mu_B^2\mu^2(\text{Fe}^{2+})}{4\pi r^3} = 1.73 \cdot 10^{-23} \text{ J} \cdot \frac{\mu^2(\text{Fe}^{2+})}{x^3} \\ &\approx 1.25 \text{ K} \cdot \frac{\mu^2(\text{Fe}^{2+})}{x^3} \end{aligned} \quad (3)$$

where μ<sub>B</sub> = 9.28 · 10<sup>-24</sup> A m<sup>2</sup> is the Bohr magneton, μ (Fe<sup>2+</sup>) = 4.90, the magnetic moment of Fe<sup>2+</sup> in units of μ<sub>B</sub>, μ<sub>0</sub> = 4π · 10<sup>-7</sup> is the permeability of the vacuum, and x is the distance in angströms between the dipoles. Since dipole-dipole interactions vary as 1/x<sup>3</sup>, they are long-range in nature. Although dipolar interactions have been shown to be significant in low-dimensional systems (Panisod and Drillon 2003), a rough estimate demonstrates that this cannot explain the observed magnetic ordering in the magnetically diluted olivine and garnet systems. For instance, in andradite with a lattice constant of 12.05 Å at 100 K (Armbruster and Geiger 1993), the assumption of randomly distributed magnetic Fe<sup>3+</sup> ions in And<sub>20</sub>Gro<sub>80</sub> yields average distances between about 7 and 10 Å. Substituting these values in Equation 3, estimated T<sub>N</sub> values in the range of 8 to 3 × 10<sup>-2</sup> K are obtained, i.e., about two orders of magnitude smaller than the experimental ones. Similar results yield estimates of 2.75 × 10<sup>-2</sup> K for And<sub>20</sub>Gro<sub>80</sub> using mean field theory. In the case of olivine, a value of 4 × 10<sup>-2</sup> K for Fa<sub>10</sub>Fo<sub>90</sub> is calculated compared with the observed value of 18.6 K (calculations of R.J. Harrison, private communication). From this first-order analysis, it follows that magnetic dipole-dipole interactions cannot provide the dominating mechanism for spin ordering in crystals rich in the diamagnetic end-member component.

Alternatively, magnetic ordering may occur in the form of superparamagnetism as observed, e.g., in systems of magnetic nanoparticles embedded in non-magnetic matrices (Bedanta and Kleemann 2009). This implies, as the basic assumption, that the distribution of magnetic ions in dilute solid solutions is not random but that clustering is preferred. That is, in the more traditional sense, where nanoparticle-like magnetic aggregates are embedded in a nonmagnetic “matrix.” In other words, short-range-cation order should be present in the solid solutions. This proposal may get support by the fact that cation clustering is energetically favorable, in a thermodynamic sense, due to local superexchange within a nanoparticle-like aggregate compared to a nonmagnetic one.

In summary, one possible interpretation of all the data is that two different magnetic mechanisms may be operating across the Fe<sub>2</sub><sup>+</sup>SiO<sub>4</sub>-Mg<sub>2</sub>SiO<sub>4</sub>, Ca<sub>3</sub>(Al<sub>x</sub>Fe<sup>3+</sup><sub>1-x</sub>)<sub>2</sub>Si<sub>3</sub>O<sub>12</sub>, and (Ca<sub>x</sub>Mn<sup>2+</sup><sub>1-x</sub>)<sub>3</sub>Al<sub>2</sub>Si<sub>3</sub>O<sub>12</sub> joins. In terms of olivine, Belley et al. (2009) stated that “magnetic properties do not vary linearly with iron content.” It is notable that the observed T<sub>N</sub> behavior is independent of a particular chemical composition or crystal structure. In both the olivine and the two garnet systems, roughly at the 50:50 composition, the nature of the magnetic interactions changes from local superexchange to long-range interactions possibly between magnetic nanoparticle-like aggregates. If this proposal for T<sub>N</sub> behavior is correct, it is the first report of variable magnetic behavior for a silicate solid solution as well as magnetic cation ordering to the best of our knowledge.

**Can short-range cation order occur in garnet or olivine solid solutions?**

The question of short-range-cation order in silicate solid solutions has been addressed using <sup>27</sup>Al and <sup>29</sup>Si MAS NMR spectroscopy. It has been proposed to occur in diamagnetic pyrope-grossular garnets, (Mg<sub>x</sub>Ca<sub>1-x</sub>)<sub>3</sub>Al<sub>2</sub>Si<sub>3</sub>O<sub>12</sub> (Bosenick et al. 1995, 1999, 2000). Indeed, NMR spectroscopy is the best ex-

perimental method in terms of addressing this issue, which is by no means trivial. The experimental problem becomes even more challenging in the case of systems containing paramagnetic ions. The experiments involve the measurement of para-magnetically shifted peaks, whose position is far outside the common range of non-paramagnetic chemical shifts. The resonance assignments and their analysis are not always straightforward. The results on various garnet systems appear to be the most well understood (i.e., Palke et al. 2015; Palke and Geiger 2016). Here, at this stage of research, the spectra do not appear to show any overt or measurable short-range cation order or clustering. The NMR spectra of forsterite-rich olivines are much more complex and little can be said because the spectra show many paramagnetically shifted resonances of which nearly all cannot be assigned (McCarty et al. 2015; Stebbins et al. 2018).

### Magnetic and $T_N$ behavior in the $(\text{Fe}_x^{2+}, \text{Mn}_{1-x}^{2+})_3\text{Al}_2\text{Si}_3\text{O}_{12}$ garnet solid solution: A binary system with two paramagnetic end-members

The third garnet binary under study has two transition metals that can occur locally at the 24c position (Figs. 4a and 4d). Low-temperature single-crystal neutron (Prandl 1971) and  $^{57}\text{Fe}$  Mössbauer measurements (Murad and Wagner 1987) show that almandine undergoes a spin transition from a paramagnetic to an antiferromagnetic state. A  $\lambda$ -peak at about 9.2 K was measured via calorimetry (Anovitz et al. 1993; Dachs et al. 2012), as shown in Figure 5. The local magnetic structure of almandine in the ground state was investigated by density functional cluster calculations (Zherebetsky et al. 2012). The interactions causing the transition are complex. The spins of the  $\text{Fe}^{2+}(3d^6)$  ions at 24c of the edge-shared dodecahedra sublattice (i.e.,  $\text{Fe}^{2+}\text{-O-Fe}^{2+}$ , Fig. 4d) interact ferromagnetically via superexchange involving intermediate oxygen atoms. Two such separate sublattices are present and they interact further through another superexchange involving connecting  $\text{SiO}_4$  and  $\text{AlO}_6$  groups via  $\text{Fe}^{2+}\text{-O-(Si)-O-Fe}^{2+}$  and  $\text{Fe}^{2+}\text{-O-(Al)-O-Fe}^{2+}$  bridges. Macroscopically, the paramagnetic-antiferromagnetic transition results.

The local magnetic interactions for intermediate  $(\text{Fe}_x^{2+}, \text{Mn}_{1-x}^{2+})_3\text{Al}_2\text{Si}_3\text{O}_{12}$  garnets are most interesting because they are totally unlike the other two garnet solid solutions discussed above.  $(\text{Fe}_x^{2+}, \text{Mn}_{1-x}^{2+})_3\text{Al}_2\text{Si}_3\text{O}_{12}$  garnets show nonlinear and negative  $T_N$  behavior across the binary between  $\text{Sps}_{100}$  and  $\text{Alm}_{100}$  (Fig. 2). There is no plateauing-like behavior toward either end-member. The high-spin  $d$ -electron configurations are  $(d\uparrow^5d\downarrow^1)$  for  $\text{Fe}^{2+}$  and  $(d\uparrow^5)$  for  $\text{Mn}^{2+}$ . If both cations are present in a solid-solution crystal, this may lead to another type of magnetic interaction known as double exchange. This mechanism was first described by Zener (1951) between  $\text{Mn}^{3+}$  and  $\text{Mn}^{4+}$  in nominal  $\text{LaMnO}_3$  perovskite, whereby some  $\text{La}^{3+}$  can be replaced by divalent Ca, Ba or Sr, which are then charge balanced by  $\text{Mn}^{4+}$  (i.e.,  $\text{La}^{3+}\text{Mn}^{3+} = [\text{Ca}, \text{Ba}, \text{Sr}]^{2+}\text{-Mn}^{4+}$ ). Further analysis of the physics behind double exchange was given by Anderson and Hasegawa (1955) and de Gennes (1960). The mechanism is well known in solid-state physics and materials science, but it, as best we know, has never been reported in rock-forming minerals. It may occur in certain garnet solid solutions having two divalent magnetic cations at 24c but with different electronic configurations. For  $(\text{Fe}_x^{2+}, \text{Mn}_{1-x}^{2+})_3\text{Al}_2\text{Si}_3\text{O}_{12}$  garnets, assuming parallel alignment for

the total spins of both ions,  $\text{Fe}^{2+}(d\uparrow^5d\downarrow^1)\text{-Mn}^{2+}(d\uparrow^5)$  with  $M_s(\text{Fe}^{2+}) = +2$  and  $M_s(\text{Mn}^{2+}) = +5/2$ , the single spin-down electron of  $\text{Fe}^{2+}$  can delocalize toward  $\text{Mn}^{2+}$ , thereby stabilizing the magnetic state. Indeed, electron delocalization leads to a decrease in kinetic energy in accordance with the Heisenberg uncertainty principle. This delocalization cannot occur for antiparallel alignment of spins, which is  $\text{Fe}^{2+}(d\uparrow^5d\downarrow^1)\text{-Mn}^{2+}(d\downarrow^5)$  with  $M_s(\text{Fe}^{2+}) = +2$  and  $M_s(\text{Mn}^{2+}) = -5/2$  and would be inconsistent with the Pauli exclusion principle. Consequently, the ferromagnetic and the stronger total antiferromagnetic interaction energy observed in  $\text{Alm}_{100}$  ( $T_N = 9.2$  K) and  $\text{Sps}_{100}$  ( $T_N = 6.2$  K) is weakened in the solid solution. Thus,  $T_N$  shows negative deviations from linearity between both end-member garnets for intermediate compositions (Fig. 2).

If magnetic double exchange does occur in  $(\text{Fe}_x^{2+}, \text{Mn}_{1-x}^{2+})_3\text{Al}_2\text{Si}_3\text{O}_{12}$  garnets, not only is the magnetic energy lowered but also the total energy of the system, albeit very slightly. It follows that there must be a thermodynamic driving force, again very slight, that maximizes the number of local  $\text{Fe}_x^{2+}\text{-Mn}_{1-x}^{2+}$  groupings (i.e., anti-clustering). In other words, there would be unfavorable energetics against forming almandine- or spessartine-like clusters.

### Effect of “impurity” atoms on $T_N$

Some of the minor scatter in  $T_N$  values for almandine-spessartine garnets (Geiger and Rossman 1994; Geiger and Feenstra 1997), or any garnet for that matter, may result from small amounts of “extra” cations that are not included in the ideal crystal-chemical formulas. Early indications of this are observable in the  $^{57}\text{Fe}$  Mössbauer spectra of almandine (Murad and Wagner 1987) and inelastic neutron scattering results on andradite (Plakhty et al. 1993).  $T_N$  of synthetic almandine can be shifted to slightly lower temperatures by the presence of small amounts of octahedral  $\text{Fe}^{3+}$  (Dachs et al. 2012). The measurable effect of “impurity” atoms in small concentrations on  $T_N$  in garnet is apparently confirmed.

This is of note because small concentrations of octahedral  $\text{Fe}^{3+}$  occur in many synthetic and natural almandine crystals (Murad and Wagner 1987; Geiger et al. 1988; Quartieri et al. 1993; Woodland et al. 1995). Furthermore, at high pressure there is complete solid solution between almandine and skiaegite, ideally  $\text{Fe}_2^{3+}\text{Fe}_3^{2+}\text{Si}_3\text{O}_{12}$  (Woodland and O’Neill 1993), and, here, the magnetic interactions can be expected to be highly complex.

### Magnetic interactions and transitions: Their effect on macroscopic thermodynamic properties and the role of crystal chemistry

**Compositionally end-member silicates.** Both olivines and garnets are orthosilicates, but they are fundamentally different in terms of the crystal structure. Fayalite has considerably stronger magnetic interactions than garnet, by nearly an order of magnitude. Indeed, the magnons associated with the magnetic phase transition in end-member fayalite at 65 K contribute more to  $C_p(T)$  than phonons between 0 K and about 70 K (Dachs et al. 2007). The relatively energetic magnons derive from the closed-packed olivine structure in which the  $\text{Fe}^{2+}$  cations are relatively close to each other in M1 and M2 polyhedra, and the cations can interact magnetically in several ways (Fig. 3). The two coordination octahedra have shared edges and corners. In

fayalite, magnons contribute significantly to the macroscopic thermodynamic behavior at standard conditions. The standard third-law entropy,  $S^\circ$ , of a crystal is given by:

$$S^\circ - S^{T=0K} \text{ J / (mol}\cdot\text{K)} = \int_0^{298.15 \text{ K}} \frac{C_p}{T} dT \quad (4)$$

assuming  $S^{T=0K} = 0$ . For fayalite  $S_{\text{mag}}(298.15 \text{ K})$  is 26.2 J/(mol·K) and it contributes about 17% to  $S^\circ$  that is equal to 151.4 J/(mol·K) (Dachs et al. 2007).

In the case of end-member garnet with transition-metal cations occurring just at the octahedral site, superexchange interactions are mediated through diamagnetic  $\text{SiO}_4$  and/or  $\text{XO}_8$  groups (Fig. 4). Thus, the interactions are very weak and magnons occur at very low energies. Andradite is a case in point. The modeled  $S_{\text{mag}}(298.15 \text{ K})$  is 28.1 J/(mol·K) and it contributes about 9% to  $S^\circ$  that is 325.0 J/(mol·K) (Geiger et al. 2018).

For garnets with transition-metal cations just at the dodecahedral site, the magnetic interactions appear to be even more subtle and complex. The total magnetic interactions involve diamagnetic  $\text{SiO}_4$  and  $\text{AlO}_6$  groups, and they do not occur directly between edge-shared dodecahedra (Zherebetsky et al. 2012), as might be expected from a first-order crystal-chemical analysis. Thus, the corresponding magnon energies are also weaker than in fayalite. For almandine, the modeled  $S_{\text{mag}}(298.15 \text{ K})$  is 32.1 J/(mol·K) and it contributes roughly 10% to  $S^\circ$ , that is 336.7 J/(mol·K) (Dachs et al. 2012). For spessartine, the model  $S_{\text{mag}}(298.15 \text{ K})$  is about 38 J/(mol·K) and  $S^\circ$  is 335.3 J/(mol·K) (Dachs et al. 2009), thus making up about 11% of the latter. The relevant equation giving the theoretical  $S_{\text{mag}}$  value is:

$$S_{\text{mag}} = R \ln(2S + 1) \text{ per mole per cation in the formula unit} \quad (5)$$

where  $R$  is the gas constant and  $(2S + 1)$  is the multiplicity, i.e., the number of electron spin orientations. Only for andradite and fayalite is the agreement between model and theoretical  $S_{\text{mag}}$  values reasonable or good.

What can be stated, further, in terms of magnetic and  $C_p(T)$  and  $S(T)$  behavior? Various purely empirical  $C_p$  models, such as corresponding states formulations (Anovitz et al. 1993; Lau et al. 2009), or more “seemingly” rigorous lattice-dynamic-type calculations (Pilati et al. 1996; Gramaccioli 2002; Gramaccioli and Pilati 2003), including neutron scattering measurements (Mittal et al. 2000), have been undertaken on garnet. Their soundness, especially, in the former cases is questionable. We have been using the simplified lattice dynamic formulation of Komada (1986) and Komada and Westrum (1997) to model  $C_{p,\text{vib}}(T)$  and  $S_{\text{vib}}(T)$  behavior, where “vib” stands for vibrational, using experimental calorimetric  $C_p^{\text{cal}}(T)$  results as input data. If the two former functions can be modeled properly,  $C_{p,\text{mag}}(T)$  and  $S_{\text{mag}}(T)$  contributions can be obtained from the difference in values [e.g.,  $C_{p,\text{mag}}(T) = C_p^{\text{cal}}(T) - C_{p,\text{vib}}(T)$ ; see Dachs et al. 2009, 2012, 2014a, 2014b; Geiger et al. 2018, for more detail]. An assumption of this model is that there are no or very minor phonon-magnon interactions. It turns out in some cases (i.e., almandine and spessartine) that the model  $S_{\text{mag}}(298.15 \text{ K})$  values are less than those obtained via Equation 5. One possibility that could explain the discrepancy is that phonon-magnon coupling is occurring. Research in this direction is needed.

**Substitutional solid-solution silicates.** The results of this investigation may help in yet another area involving thermodynamic properties (Geiger 2001). It involves macroscopic thermodynamic mixing behavior, namely  $\Delta C_p^{\text{mix}}(T)$  and  $\Delta S^{\text{mix}}(T)$ , for solid solutions containing a transition metal ion or ions (see Dachs et al. 2007, 2014a, 2014b; Dachs and Geiger 2019). In short, a precise determination of  $\Delta C_p^{\text{mix}}(T)$  and  $\Delta S^{\text{mix}}(T)$  behavior, obtained from an application of the Komada and Westrum (1997) model, can be problematic if they are small in magnitude. However,  $T_N$  behavior for a solid solution can help qualitatively in this question, because it can be measured precisely, and it is not in any respect model dependent. Consider the system olivine (Fig. 1). Dachs et al. (2007) argued that  $\Delta S_{\text{mag}}^{\text{mix}}(298.15 \text{ K})$  behavior shows slight negative deviations from ideality across the  $\text{Fe}_2^+\text{SiO}_4\text{-Mg}_2\text{SiO}_4$  join (i.e.,  $\Delta S_{\text{mag}}^{\text{mix}} < 0$ ).  $T_N$  behavior shows as well negative deviations from linearity (Fig. 1) between  $\text{Fa}_{100}$  and  $\text{Fa}_{10}\text{Fo}_{90}$ . It must be noted, on the other hand, that a similar relationship does not appear to exist for andradite-grossular or spessartine-grossular garnets, where in both cases  $\Delta S_{\text{mag}}^{\text{mix}}(298.15 \text{ K}) = 0$ .

## IMPLICATIONS

An understanding of the magnetic behavior of silicates, and especially their solid solutions, in both a solid-state physical and mineralogical context, is in its infancy. Little is known, and much research remains to be done. Several significant implications can be drawn from this first investigation on olivine and garnet.

First, we conclude that the observed  $\lambda$ -anomaly in the low-temperature  $C_p(T)$  results on synthetic uvarovite,  $\text{Ca}_3\text{Cr}_2^+\text{Si}_3\text{O}_{12}$ , and knorringite,  $\text{Mg}_3\text{Cr}_2^+\text{Si}_3\text{O}_{12}$  (Klemme et al. 2005; Wijbrans et al. 2014) is caused by a paramagnetic-antiferromagnetic transition. It must be expected that most, if not all, transition-metal-bearing silicate and germanium garnets will have very low-temperature magnetic spin transitions. This may be true for other silicates as well. A determination of their heat-capacity and magnetic behavior will require measurements down to the lowest possible temperatures. This was not always done in the past, and it led to incorrect results (see the case for andradite, Geiger et al. 2018).

Second, it can be proposed that double-exchange interactions may occur among other magnetic ions than just between  $\text{Fe}^{2+}$  and  $\text{Mn}^{2+}$ . In terms of garnet, it may occur, for example, between  $\text{Fe}^{2+}$  at 24c and  $\text{Fe}^{3+}$  at 16a in garnet. For example, double exchange may possibly occur in certain andradites and almandines, where  $C_p$  results show small variations in  $T_N$  and  $\lambda$ -anomaly behavior among different crystals (Dachs et al. 2012; Geiger et al. 2018). Furthermore, several rock-forming silicate systems show an exchange between  $\text{Fe}^{2+}$  and  $\text{Mn}^{2+}$  and, here, magnetic double exchange may occur. This goes, for example, for the fayalite-tephroite ( $\text{Mn}_2\text{SiO}_4$ ) join (Burns and Huggins 1972). Marked exchange of  $\text{Mn}^{2+}\text{-Fe}^{2+}\text{-(Mg)}$  cations occurs in pyroxenes, amphiboles, and micas. In all these silicates,  $\text{Mn}^{2+}$  and  $\text{Fe}^{2+}$  can be found in corner- and edge-shared octahedral sites and, thus,  $d$ -electron delocalization could be expected.

Finally, and almost needless to say, the precise magnetic behavior of many solid-solution silicates, containing two or more different transition-metal cations, may prove to be complex in nature. Their low-temperature  $C_p$  and magnetic behavior can be

expected to be complicated by virtue of the range of possible chemistries and structural sites. The number of different local-electron-spin interactions is expected to be large.

### FUNDING AND ACKNOWLEDGMENTS

E.C. Ferré (Lafayette, Louisiana) kindly supplied the data from the magnetic susceptibility measurements on olivine. This study was supported by a grant to C.A.G. from the Austrian Science Fund (FWF: P 30977-NBL). C.A.G. also thanks the “Land Salzburg” for financial support through the initiative “Wissenschafts- und Innovationsstrategie Salzburg 2025”. We thank the two referees, and especially R.J. Harrison (Cambridge, U.K.), whose keen review encouraged us to consider more fully the possible role of superparamagnetism instead of dipole-dipole interactions in the solid solutions. The editor S. Speziale (Potsdam, Germany) also provided useful remarks on improving the clarity of the manuscript.

I (C.A.G.) first met John Valley at the University of Michigan years ago, where I was an undergraduate and John a graduate student in the Department of Geological Sciences. The electron microprobe was located in the Engineering Department and I had technical difficulties with the machine working completely alone late one night (lowly students only received measuring time on the night shift). I ran, almost in a panic, back to the Geology Department hoping to find someone there who could help me out. John was working in his office, as often was the case, and he came to the rescue. I dedicate, now, this manuscript to him.

### REFERENCES CITED

- Anderson, P.W., and Hasegawa, H. (1955) Considerations on double exchange. *Physical Review*, 100, 675–681.
- Anovitz, L.M., Essene, E.J., Metz, G.W., Bohlen, S.R., Westrum, E.F. Jr., and Hemingway B.S. (1993) Heat capacity and phase equilibria of almandine,  $\text{Fe}_3\text{Al}_2\text{Si}_5\text{O}_{12}$ . *Geochimica et Cosmochimica Acta*, 57, 4191–4204.
- Armbruster, T., and Geiger, C.A. (1993) Andradite crystal chemistry, dynamic X-site disorder and strain in silicate garnets. *European Journal of Mineralogy*, 5, 59–71.
- Armbruster, T., Geiger, C.A., and Lager, G.A. (1992) Single crystal X-ray refinement of almandine-pyrope garnets at 298 and 100 K. *American Mineralogist*, 77, 512–523.
- Aronson, M.C., Stixrude, L., Davis, M.K., Gannon, W., and Ahilan, K. (2007) Magnetic excitations and heat capacity of fayalite,  $\text{Fe}_2\text{SiO}_4$ . *American Mineralogist*, 92, 481–490.
- Bedanta, S., and Kleemann, W. (2009) Supermagnetism. *Journal of Physics D, Applied Physics*, 42, 1–28.
- Belley, F., Ferré, E.C., Fátima, M-H., Jackson, M.J., Dyar, M.D., and Catlos, E.J. (2009) The magnetic properties of natural and synthetic  $(\text{Fe}_x\text{Mg}_{1-x})_2\text{SiO}_4$  olivines. *Earth and Planetary Sciences Letters*, 284, 516–526.
- Blundell, S. (2001) Magnetism in Condensed Matter, 238 p. Oxford.
- Bosenick, A., Geiger, C.A., Schaller, T., and Sebald, A. (1995) An  $^{29}\text{Si}$  MAS NMR and IR spectroscopic investigation of synthetic pyrope-grossular garnet solid solutions. *American Mineralogist*, 80, 691–704.
- Bosenick, A., Geiger, C.A., and Phillips, B. (1999) Local Ca-Mg distribution of Mg-rich pyrope-grossular garnets synthesized at different temperatures revealed by  $^{29}\text{Si}$  NMR MAS spectroscopy. *American Mineralogist*, 84, 1422–1433.
- Bosenick, A., Dove, M.T., and Geiger, C.A. (2000) Simulation studies of pyrope-grossular solid solutions. *Physics and Chemistry of Minerals*, 27, 398–418.
- Burns, R.G., and Huggins, F.E. (1972) Cation determinative curves for Mg-Fe-Mn olivines from vibrational spectra. *American Mineralogist*, 57, 967–985.
- Cococcioni, M., Dal Corso, A., and de Gironcoli, S. (2003) Structural, electronic, and magnetic properties of  $\text{Fe}_2\text{SiO}_4$  fayalite: Comparison of LDA and GGA results. *Physical Review B*, 67, 094106, 7 p.
- Dachs, E., and Geiger, C.A. (2019) Thermodynamic behavior of grossular-andradite,  $\text{Ca}_3(\text{Al,Fe}^{2+})_2\text{Si}_5\text{O}_{12}$ , garnets: A calorimetric study. *European Journal of Mineralogy*. DOI: 10.1127/ejm/2019/0031-2827.
- Dachs, E., Geiger, C.A., von Seckendorff, V., and Grodzicki, M. (2007) A low-temperature calorimetric study of synthetic forsterite-fayalite ( $\text{Mg}_2\text{SiO}_4$ - $\text{Fe}_2\text{SiO}_4$ ) solid solutions: An analysis of vibrational, magnetic and electronic contributions to the molar heat capacity and entropy of mixing. *Journal of Chemical Thermodynamics*, 39, 906–933.
- Dachs, E., Geiger, C.A., Withers, A.C., and Essene, E.J. (2009) A calorimetric investigation of spessartine: Vibrational and magnetic heat capacity. *Geochimica et Cosmochimica Acta*, 73, 3393–3409.
- Dachs, E., Geiger, C.A., and Benisek, A. (2012) Almandine: Lattice and non-lattice heat capacity behavior and standard thermodynamic properties. *American Mineralogist*, 97, 1171–1182.
- (2014a) Thermodynamic mixing properties and behavior of grossular-spessartine,  $(\text{Ca}_x\text{Mn}_{1-x})_3\text{Al}_2\text{Si}_5\text{O}_{12}$ , solid solutions. *Geochimica et Cosmochimica Acta*, 141, 294–302.
- Dachs, E., Geiger, C.A., Benisek, A., and Grodzicki, M. (2014b) Thermodynamic mixing properties and behavior of almandine-spessartine solid solutions. *Geochimica et Cosmochimica Acta*, 125, 210–224.
- de Gennes, P.G. (1960) Effects of double exchange in magnetic crystals. *Physical Review*, 118, 141–154.
- Geiger, C.A. (2000) Volumes of mixing in aluminosilicate garnets: Implications for solid solution behavior. *American Mineralogist*, 85, 893–897.
- Ed. (2001) Oxide and Silicate Solid Solutions of Geological Importance. European Mineralogical Union Notes in Mineralogy, vol. 3, 465 p. Eötvös University Press.
- (2013) Garnet: A key phase in nature, the laboratory and in technology. *Elements*, 9, 447–452.
- Geiger, C.A., and Feenstra, A. (1997) Molar volumes of mixing of almandine-pyrope and almandine-spessartine garnets and the crystal chemistry of aluminosilicate garnets. *American Mineralogist*, 82, 571–581.
- Geiger, C.A., and Rossman, G.R. (1994) Crystal field stabilization energies of almandine-pyrope and almandine-spessartine garnets determined by FTIR near infrared measurements. *Physics and Chemistry of Minerals*, 21, 516–525.
- Geiger, C.A., Langer, K., Winkler, B., and Cemic, L. (1988) The synthesis, characterization and physical properties of end-member garnets in the system  $(\text{Fe,Mg,Ca,Mn})_3\text{Al}_2(\text{SiO}_4)_3$ . In H. Vollstädt, Ed., High Pressure Geosciences and Material Synthesis, Proceedings XXV. Annual Meeting European High Pressure Research Group, p. 193–198. Akademie-Verlag.
- Geiger, C.A., Dachs, E., Vielreicher, N., and Rossman, G.R. (2018) Heat capacity behavior of andradite: A multi-sample and -methodological investigation. *European Journal of Mineralogy*, 30, 681–694.
- Geller, S. (1967) Crystal chemistry of garnets. *Zeitschrift für Kristallographie*, 125, 1–47.
- Goodenough, J.B. (1963) Magnetism and the Chemical Bond, 393 p. Wiley.
- Gopal, E.S.R. (1966) Specific Heats at Low Temperatures, 240 p. Plenum Press.
- Gramaccioli, C.M. (2002) Lattice dynamics: Theory and application to minerals. In C.M. Gramaccioli, Ed., Energy Modelling in Minerals, 4, p. 245–270. European Mineralogical Union Notes in Mineralogy, European Mineralogical Union, Vienna, Austria.
- Gramaccioli, C.M. and Pilati, T. (2003) Interpretation of single-crystal vibrational spectra and entropy of pyrope and almandine using a rigid-ion lattice-dynamical model. *Journal of Physical Chemistry*, 107, 4360–4366.
- Grimvall, G. (1986) Thermophysical Properties of Materials, 348 p. Elsevier.
- Heinemann, R., Kroll, H., Kirfel, A., and Barbier, B. (2007) Order and anti-order in olivine III: Variation of the cation distribution in the Fe,Mg olivine solid solution series with temperature and composition. *European Journal of Mineralogy*, 19, 15–27.
- Klemme, S., van Miltenburg, J.C., Javorsky, P., and Wastin, F. (2005) Thermodynamic properties of uvarovite garnet  $\text{Ca}_3\text{Cr}_2\text{Si}_5\text{O}_{12}$ . *American Mineralogist*, 90, 663–665.
- Kolesov, B.A., and Geiger, C.A. (2004) A temperature-dependent single-crystal Raman spectroscopic study of fayalite: evidence for phonon-magnetic excitation coupling. *Physics and Chemistry of Minerals*, 31, 155–161.
- Komada, N. (1986) Measurement and interpretation of heat capacities of several inorganic substances. Ph.D. thesis, Department of Chemistry, University of Michigan, 384 p.
- Komada, N., and Westrum, E.F. (1997) Modeling lattice heat capacity contributions by a single-parametric phonon dispersion approach. *Journal of Chemical Thermodynamics*, 29, 311–336.
- Lau, G.C., Klimczuk, T., Ronning, F., McQueen, T.M., and Cava, R.J. (2009) Magnetic properties of the garnet and glass forms of  $\text{Mn}_3\text{Al}_2\text{Si}_5\text{O}_{12}$ . *Physical Review B*, 80, 21441(5).
- Lottermoser, W., Müller, R., and Fuess, H. (1986) Antiferromagnetism in synthetic olivines. *Journal of Magnetism and Magnetic Materials*, 54-57, 1005–1006.
- McCarty, R.J., Palke, A.C., Stebbins, J.F., and Hartman, J.S. (2015) Transition metal cation site preferences in forsterite ( $\text{Mg}_2\text{SiO}_4$ ) determined from paramagnetically shifted NMR resonances. *American Mineralogist*, 100, 1265–1276.
- Menzer, G. (1928) Die Kristallstruktur der Granate. *Zeitschrift für Kristallographie*, 69, 300–396.
- Meyer, A., Pascale, F., Zicovich-Wilson, C.M., and Dovesi, R. (2010) Magnetic interactions and electronic structure of uvarovite and andradite garnets. An ab-initio all-electron simulation with the program Crystal06 program. *International Journal of Quantum Chemistry*, 110, 338–351.
- Mittal, R., Chaptal, S.L., Choudhury, N., and Loong, C.-K. (2000) Inelastic neutron scattering and lattice-dynamics studies of almandine  $\text{Fe}_3\text{Al}_2\text{Si}_5\text{O}_{12}$ . *Physical Review B*, 61, 3983–3988.
- Müller, R., Fuess, H., and Brown, P.J. (1982) Magnetic properties of synthetic fayalite ( $\alpha\text{-Fe}_2\text{SiO}_4$ ). *Journal de Physique Colloques*, 43, C7-249–252.
- Murad, E. (1984) Magnetic ordering in andradite. *American Mineralogist*, 69, 722–724.
- Murad, E., and Wagner, F.E. (1987) The Mössbauer spectrum of almandine. *Physics and Chemistry of Minerals*, 14, 264–269.
- Néel, M.L. (1948) Propriétés magnétiques des ferrites; ferrimagnétisme et antiferromagnétisme. *Annales de Physique*, 12, 137–198.
- Novak, G.A., and Gibbs, G.V. (1971) The crystal chemistry of the silicate garnets. *American Mineralogist*, 56, 791–825.
- Palke, A.C., and Geiger, C.A. (2016) Trivalent transition-metal cations and local structure in synthetic pyrope- and grossular-rich solid solutions investigated by  $^{27}\text{Al}$  and  $^{29}\text{Si}$  MAS NMR spectroscopy. *European Journal of Mineralogy*,

- 28, 179–187.
- Palke, A.C., Stebbins, J.F., Geiger, C.A., and Tippelt, G. (2015) Cation order-disorder in Fe-bearing pyrope and grossular garnets: An  $^{27}\text{Al}$  and  $^{29}\text{Si}$  MAS NMR and  $^{57}\text{Fe}$  Mössbauer spectroscopy study. *American Mineralogist*, 100, 536–547.
- Panissod, P., and Drillon M. (2003) Magnetic ordering due to dipolar interaction in low dimensional materials. In J.S. Miller and M. Drillon, Eds., *Magnetism: Molecules to Materials IV*, p. 233–270. Wiley-VCH.
- Parks, G.A., and Akhtar, S. (1968) Magnetic moment of  $\text{Fe}^{2+}$  in paramagnetic minerals. *American Mineralogist*, 53, 406–415.
- Pilati, T., Demartin, F., and Gramaccioli, C.M. (1996) Atomic displacement parameters for garnets: A lattice-dynamical evaluation. *Acta Crystallographica*, B52, 239–250.
- Plakhty, V., Golosovsky, I., Gukasov, A., Smirnov, O., Brückel, T., Dorner, B., and Burlet, P. (1993) Spin waves and exchange interactions in the antiferromagnetic garnets with  $\text{Fe}^{3+}$  in the octahedral sites. *Zeitschrift für Physik B*, 92, 443–449.
- Prandl, W. (1971) Die magnetische Struktur und die Atomparameter des Almandins  $\text{Al}_2\text{Fe}_3(\text{SiO}_4)_3$ . *Zeitschrift für Kristallographie*, 134, 333–343.
- (1973) Rhombohedral magnetic structure of spessartine type garnets. *Physica status solidi b*, 55, K159–163.
- Quartieri, S., Artioli, G., Deriu, A., Lottici, P.P., and Antonioli, G. (1993)  $^{57}\text{Fe}$ -Mössbauer investigation on garnets from the Ivrea-Verbano zone. *Mineralogical Magazine*, 57, 671–676.
- Robie, R.A., Finch, C.B., and Hemingway, B.S. (1982) Heat capacity and entropy of fayalite ( $\text{Fe}_2\text{SiO}_4$ ) between 5.1 and 383 K: comparison of calorimetric and equilibrium values for the QFM buffer reaction. *American Mineralogist*, 67, 463–469.
- Rodehorst, U., Carpenter, M.A., Boffa Ballaran, T., and Geiger, C.A. (2004) Local structural heterogeneity, mixing behaviour and saturation effects in the grossular-spessartine solid solution. *Physics and Chemistry of Minerals*, 31, 387–404.
- Santoro, R.P., Newnham, R.E., and Nomura, S. (1966) Magnetic properties of  $\text{Mn}_2\text{SiO}_4$  and  $\text{Fe}_2\text{SiO}_4$ . *Journal of Physical and Chemistry of Solids*, 27, 655–666.
- Stebbins, J.F., McCarty, R.J., and Palke, A.C. (2018) Toward the wider application of  $^{29}\text{Si}$  NMR spectroscopy to paramagnetic transition metal silicate minerals and glasses: Fe(II), Co(II), and Ni(II) silicates. *American Mineralogist*, 103, 776–791.
- Stout, J.W. (1961) Magnetic transitions at low temperatures. *Pure and Applied Chemistry*, 1–2, 287–296.
- von Seckendorff, V., and O'Neill, H.St.C. (1993) An experimental study of Fe-Mg partitioning between olivine and orthopyroxene at 1173, 1273 and 1423 K and 1.6 GPa. *Contributions to Mineralogy and Petrology*, 113(2), 196–207.
- Wijbrans, C.H., Neihaus, O., Rohrbach, A., Pöttgen, R., and Klemme, S. (2014) Thermodynamic and magnetic properties of knorringite garnet ( $\text{Mg}_3\text{Cr}_2\text{Si}_5\text{O}_{12}$ ) based on low-temperature calorimetry and magnetic susceptibility measurements. *Physics and Chemistry of Minerals*, 41, 341–346.
- Winkler, G. (1981) *Magnetic Garnets*, 735 p., vol. 5. Vieweg und Sohn, Braunschweig/Wiesbaden, BRD.
- Woodland, A.B., and O'Neill, H.St.C. (1993) Synthesis and stability of  $\text{Fe}_3^{2+}\text{Al}_3^{3+}\text{Si}_5\text{O}_{12}$  garnet and phase relations with  $\text{Fe}_3\text{Al}_2\text{Si}_5\text{O}_{12}$ - $\text{Fe}_3^{2+}\text{Fe}_3^{3+}\text{Si}_5\text{O}_{12}$  solutions. *American Mineralogist*, 78, 1000–1013.
- Woodland, A.B., Droop, G., and O'Neill, H.St.C. (1995) Almandine-rich garnet from Collobrières, southern France, and its petrological significance. *European Journal of Mineralogy*, 7, 187–194.
- Zener, C. (1951) Interaction between the *d*-shells in the transition metals. II. Ferromagnetic compounds of manganese with perovskite structure. *Physical Review*, 82, 403–440.
- Zherebetskyy, D., Lebernegg, S., Amthauer, G., and Grodzicki, M. (2012) Magnetic structure of almandine. *Physics and Chemistry of Minerals*, 39, 351–361.

MANUSCRIPT RECEIVED OCTOBER 8, 2018

MANUSCRIPT ACCEPTED APRIL 9, 2019

MANUSCRIPT HANDLED BY SERGIO SPEZIALE

### Endnote:

<sup>1</sup>Deposit item AM-19-96839, Supplemental Figure. Deposit items are free to all readers and found on the MSA website, via the specific issue's Table of Contents (go to [http://www.minsocam.org/MSA/AmMin/TOC/2019/Sep2019\\_data/Sep2019\\_data.html](http://www.minsocam.org/MSA/AmMin/TOC/2019/Sep2019_data/Sep2019_data.html)).